



ELSEVIER

Contents lists available at ScienceDirect

# Nuclear Instruments and Methods in Physics Research A

journal homepage: [www.elsevier.com/locate/nima](http://www.elsevier.com/locate/nima)

## Chopper layout for spectrometers at long pulse neutron sources



J. Voigt\*, N. Violini, T. Brückel

Jülich Centre for Neutron Science JCNS and Peter Grünberg Institut PGI, JARA-FIT Forschungszentrum Jülich GmbH, 52425 Jülich, Germany

### ARTICLE INFO

#### Article history:

Received 14 May 2013

Received in revised form

16 December 2013

Accepted 16 December 2013

Available online 25 December 2013

#### Keywords:

Neutron spectroscopy

Neutron choppers

Time-of-flight spectroscopy

### ABSTRACT

We discuss the implications of a long pulse neutron source for the chopper system of direct geometry time-of-flight spectrometers. While the same conditions apply for the layout of the resolution defining choppers as on reactor based instruments, we emphasize the multi-chromatic nature of the instruments. The chopper system must not only provide a unique assignment of the wavelength to each pulse, but also provide adopted time frames matching the respective energy of the pulse. We propose a chopper system consisting of disc choppers, heavy TO choppers and a newly developed Fan chopper to account for the various challenges due to the long pulse nature.

© 2014 Elsevier B.V. All rights reserved.

## 1. Introduction

Direct geometry neutron time-of-flight spectrometers have been used traditionally for high resolution studies of self-correlation functions and local excitations, which give rise to scattering into a large solid angle. These and similar studies do not require high momentum space resolution due to the small dispersion and therefore the instrument can measure the scattering signals with a high efficiency by large solid angle coverage of the detector. For the measurements of coherent inelastic scattering traditionally three axis neutron spectroscopy has been employed. With the development of large position sensitive detectors and the improvement of the instrument brilliance it became possible to map the reciprocal space of single crystalline samples efficiently with chopper spectrometers thanks to the large detector coverage. The most prominent early example of this application is the MAPS spectrometer at the short pulse spallation source ISIS, which was followed by instruments at the new MW spallation sources SNS and J-Parc. These instruments benefit from the high peak brilliance of the source. Due to the short neutron pulses the time-of-flight resolution is extremely good. The latest generation of reactor based time-of-flight spectrometers has adopted the mapping capabilities. The lower peak flux of the moderator spectrum is partly compensated by higher measurement frequencies or repetition rate as compared to the spallation source, at least for moderate resolution requirements. While at steady sources repetitions rates up to 1000 Hz can be realized, spallation sources typically run at frequencies from 10 to 60 Hz. The frequency

limitation has been overcome by multi-chromatic use of the spallation source, sometimes called the Repetition Rate Multiplication (RRM) [1] or Multiple  $E_i$  method [2]. At the future long pulse spallation source ESS, the multi-chromatic methods have to be explored for all instruments in order to use the neutrons from the source efficiently and explore the potential gain in instrument performance due to the increased peak brightness. In this paper we describe the implications on the chopper system for the multi-chromatic operation. It is organized as follows: first we review the relationship between energy resolution and intensity with respect to the requests for the chopper system. Then we discuss the novel challenges for an improved multi-chromatic operation. We briefly discuss the problem of the long pulse in terms of background and the layout of a TO chopper. Finally we conclude with recommendations for the layout of chopper systems serving different applications.

## 2. Energy resolution

In direct geometry time-of-flight spectroscopy the neutron velocity is selected by the M chopper (counter rotating chopper pair) that transmits only the neutrons of a pulse, that have the desired velocity. The neutron pulse itself can be formed either by the source as in the case of a short pulse spallation source or by (pair of) choppers as on reactor based TOF spectrometers, the so-called P chopper. The generic layout of a direct geometry time-of-flight spectrometer for a reactor source and also for a long pulse source is shown in Fig. 1.

The energy resolution can be calculated from the apparent time spread due to the finite pulse width  $\tau_P$  and  $\tau_M$  at the P chopper and the M chopper, respectively. While these two contributions to the energy resolution are experimentally controlled by the

\* Corresponding author.

E-mail address: [j.voigt@fz-juelich.de](mailto:j.voigt@fz-juelich.de) (J. Voigt).

chopper system, flight path uncertainties due to the spatial extension of the neutron beam and the sample and due to the time and the position of the neutron detection have to be taken

into account [3,4].

$$\Delta E = \frac{h^3 \sqrt{A^2 + B^2 + C^2}}{m_n^2 \lambda'^3 L_{SD} L_{PM}} \quad (1)$$

$$A = \tau_M (L_{PM} + L_{MS} + (\lambda'/\lambda)^3 L_{SD}) \quad (2)$$

$$B = \tau_P (L_{MS} + (\lambda'/\lambda)^3 L_{SD}) \quad (3)$$

$$C = \frac{m_n}{h} L_{PM} \cdot \lambda' \cdot \Delta L \quad (4)$$

with  $\lambda, \lambda'$  representing the neutron wavelength before and after scattering at the sample, respectively. The different flight paths are introduced in Fig. 1.  $\tau_P$  and  $\tau_M$  give the opening times of the P and M chopper, respectively. Also the intensity  $I$  that passes through a chopper system is proportional to the pulse width and the geometry of the instrument

$$I \propto \frac{\tau_P \tau_M}{L_{PM} L_{SD}} \quad (5)$$

The optimization of the energy resolution under the additional condition of maximized intensity relates the burst times of the P and M choppers, respectively:

$$\tau_P = \tau_M \left( \frac{L_{PM}}{L_{MS} + (\lambda'/\lambda)^3 L_{SD}} + 1 \right) \quad (6)$$

i.e. when the uncertainty contributions  $A$  and  $B$  are equal.

In the flight path diagram Fig. 1 the chopper openings  $\tau_P, \tau_M$  and the distance between the choppers  $L_{PM}$  determine the velocity distribution, which can pass through the chopper system. Also the energy transfer resolution is completely determined by the P and M chopper system, if the appropriate flight path uncertainties are taken into account. We emphasize here that the contribution of the flight path uncertainty is directly proportional to the final wavelength  $\lambda'$ . If the final wavelength is short, this contribution can therefore be neglected while it becomes dominating for long wavelength. Particularly for thermal neutrons and for neutron energy gain processes short pulses define therefore the performance of the instrument. For long final neutron wavelength  $\lambda'$  it is however necessary to keep the flight path uncertainties as small as possible. From Eq. (6) we see that the requirements on the P chopper burst time are more relaxed than the requirements on the M chopper, if the distance between the choppers is significantly larger than the sample-to-detector distance  $L_{SD}$  and the monochromator-to-sample distance  $L_{MS}$ . The major technological challenge is therefore the matching of the M chopper contribution and the flight path uncertainties. Using counter rotating chopper pairs and multi-slit configurations [5] as used on the LET

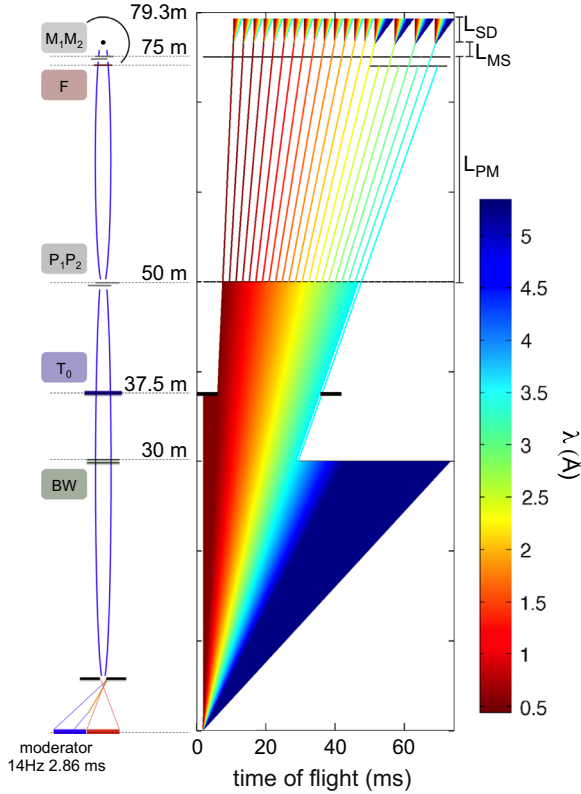


**Fig. 1.** Generic layout of a chopper spectrometer and a schematic flight path diagram showing the action of the choppers for a total instrument length  $L_{Det} = 79.3$  m. Neutrons are emitted from the moderator during the pulse length of the source. Different colors code the neutron wavelength before and after scattering  $\lambda$  and  $\lambda'$ , respectively. The initial  $\lambda$  is calculated using the emission time at the moderator, from which the P and M choppers accept neutrons. For a discussion of the consequences of the extended pulse see Figs. 3, 4 and 6. The neutron pulse is shaped by the P chopper and a narrow velocity/wavelength distribution is selected by the M chopper. The additional choppers avoid cross-talk between the different chopper/source pulses (bandwidth choppers 'BW'), time frame overlap (the newly developed fan chopper 'F' consisting of multiple blades) and block the direct line-of-sight, when the proton pulse interacts with the target (T0 chopper). (For interpretation of the references to color in this figure caption, the reader is referred to the web version of this paper.)

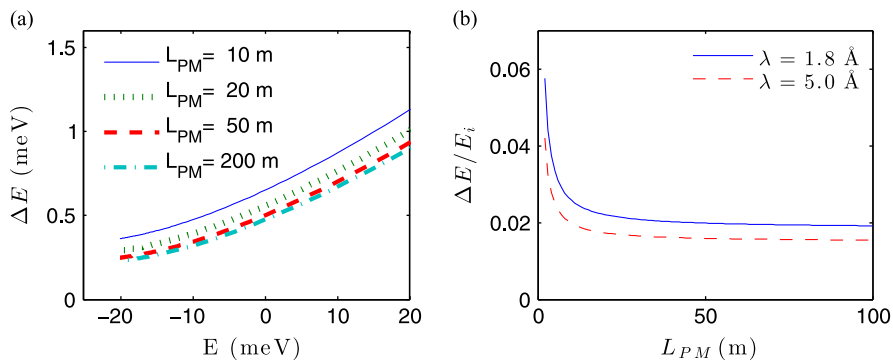


**Fig. 2.** (a) Energy resolution for different distances  $L_{PM}$  for balanced P and M choppers, assuming a flight path uncertainty  $\Delta L = 20$  mm. The initial wavelength is  $\lambda = 1.8$  Å. (b) Energy resolution for  $h\omega = 0$  meV as a function of chopper distance  $L_{PM}$  for different initial wavelengths  $\lambda$ ,  $\tau_M = 10, 20$   $\mu$ s for the short and long wavelength, respectively. The flight path uncertainty is  $\Delta L = 20$  mm as in (a).

spectrometer at ISIS or Fermi choppers, chopper opening times of 10  $\mu\text{s}$  (FWHM) are achievable today for reasonable neutron window width of 10–20 mm. We calculate the energy resolution according to Eqs. (1)–(4) for different chopper distances  $L_{\text{PM}}$  in Fig. 2. We account for the different contribution from an assumed flight path uncertainty  $\Delta L = 20$  mm by choosing different pulse length of the M chopper and balance the pulse length of the P chopper accordingly. The resolution is improved significantly, if  $L_{\text{PM}}$  is increased from 10 to 20 m. The difference between the 50 m and 200 m case is comparably small. If instead  $\Delta L = 40$  mm is assumed, the differences become less pronounced for the 5  $\text{\AA}$  case, as the resolution is governed by the  $\Delta L$  contribution and not controllable by the chopper system anymore. Thus it is especially important to keep the flight path uncertainties small for high resolution cold chopper spectrometers, which represents a special challenge for the detector development.

### 3. Characteristic wavelengths of chopper systems at spallation sources

The mismatch between the periodicity of the spallation source (typically 20–100 ms) and the time frame  $T_{\text{frame}}$  necessary to collect the neutrons of interest for the experiment (see Eq. (11)), typically ranging from several ms to tens of ms for thermal and cold neutrons, inspired the idea of repetition rate multiplication or the multiple  $E_i$  method [1,6–8]. As seen from Fig. 1 subsequent openings of the M chopper select different wavelengths with a step size  $\delta\lambda$  from the spectrum. As each incident pulse can be used to collect a time-of-flight spectrum, such multi-chromatic operation corresponds to performing many experiments with different incident energies  $E$ . The dynamical range, which can be covered, is determined from the bandwidth  $\Delta\lambda$  set by the distance between the source and the detector  $L_{\text{Det}}$  and the source frequency  $f_{\text{source}}$ :

$$\Delta\lambda = \frac{h}{m_n} (f_{\text{source}} L_{\text{Det}})^{-1} \quad (7)$$

The wavelength stepsize  $\delta\lambda$  is given accordingly:

$$\delta\lambda = \frac{h}{m_n} (f_M L_M)^{-1} \quad (8)$$

We recall here the value of  $h/m_n = 3956 \text{ m s}^{-1} \text{ \AA}$  in practical units.  $f_M$  denotes the frequency, at which the M chopper opens, and  $L_M$  gives the distance from the moderator to the M chopper. From Eqs. (7) and (8) it is clear that large distances lead to a narrow band instrument with small wavelength or energy steps. In a sense such an instrument becomes close to an experiment at a continuous source. For short distances it becomes possible to cover a huge energy range in a single pulse. For the geometry shown in Fig. 1 the bandwidth  $\Delta\lambda$  corresponds to neutron energies ranging from 7 to 280 meV, where the upper wavelength limit is determined by the opening of the TO chopper.

To understand how the neutron source is used by the chopper system, we employ the concept of acceptance diagrams [9,10]. As introduced by Andersen [10] we chose the time as the abscissa and the wavelength as ordinate. The colored regions in Fig. 3a indicate at what time and wavelength a neutron must be emitted from the moderator surface to reach the respective chopper in an open position. To pass through the chopper system all choppers in the system have to accept the respective neutron. So neutrons, which are emitted from the source at the time with the wavelength at the crossing of the different acceptance regions, pass through the chopper system.

The repetition rates of the P and M choppers have to be linked by the distance from the source  $L_P$  and  $L_M$  to transmit the same

wavelength periodically with the source frequency:

$$f_P = \frac{L_M}{L_P} f_M \quad (9)$$

(note, that the repetition rate of a chopper can be increased by distributing several windows equidistantly on the circumference of the disk). In turn all neutrons that pass through a chopper system fulfilling condition Eq. (9) originate from the same time at the moderator surface within the resolution limits, as shown in the top of Fig. 3b. This time has been used in Fig. 1 to calculate the neutron wavelength  $\lambda$ .

As evident from Fig. 3 for large distances the acceptance region is mainly determined by the M chopper. If the overall distance of the chopper system from the source is increased, the time region, from which transmitted neutrons start, will be increased. But as the neutron pulse is also spreading more during the longer flight path, the spectral density remains the same and accordingly the transmitted intensity, assuming that the neutron transport is ideal and determines the transported divergence completely.

The time covered in Fig. 3a includes the time of the neutron pulse and 3 ms for the so-called after glow, during which neutrons will be emitted, to check for possible contamination. It shows a situation, where P and M choppers are phased in order to transmit neutrons of wavelength  $\lambda = 5 \text{ \AA}$ , which were emitted 1.9 ms after the beginning of the pulse. In addition, acceptance regions are shown for the preceding and following chopper pulses.

The wavelength step Eq. (8) is given by the distance between neighboring acceptance regions. If additional crossing regions exist during the time the source emits neutrons, the chopper system exhibits cross-talk. During one opening of the M chopper two different wavelength packages would be transmitted, which would prevent the energy analysis of the scattered neutrons. The cross-talk between different openings of the choppers is excluded for the  $L_P = 50$  m,  $L_M = 75$  m and the  $L_P = 100$  m,  $L_M = 150$  m configurations. For the chopper layout governed by Eq. (9) all common acceptance regions of the P and M chopper at the moderator originate from the same time, independent of the incoming wavelength  $\lambda$ . The distance in time to the next accepted region is independent of the incoming wavelength  $\lambda$ , too, and depends only on the distance between the P and M choppers and the distances between the choppers and the moderator. The argument given here is equivalent to the reasoning of Schober et al. [11]: the bandwidth of the chopper system consisting of the P chopper and the pulse is narrower than the repeat wavelength of the system M chopper and pulse.

For the two other configurations, the cross-talk must be considered further in the design of the chopper system, but it can also be explored to overcome condition Eq. (9). Especially for a short distance  $L_P$  the bandwidth  $\Delta\lambda_P$  is significantly larger than the step size  $\delta\lambda_M$ . So one pulse passing through the P chopper can feed several openings of the M chopper, as shown in the inset of the lower panel in Fig. 3b. The repetition rate of the P chopper can be reduced accordingly. This leads however to different originating times at the moderator for the different wavelengths  $\lambda$ . To assure, that only neutrons from the plateau region of the source pulse are accepted, the bandwidth passing through the P chopper  $\Delta\lambda_P$  must be larger than the instrument bandwidth  $\Delta\lambda$  (see Eq. (7)). Assuming a minimal distance  $L_P = 6$  m we can estimate that the distance  $L_{\text{Det}}$  from moderator to detector must be larger than 166 m, if the burst time of the P chopper  $\tau_P$  is balanced for  $\lambda' = \lambda$  and  $\tau_M = 20 \mu\text{s}$ . One has to consider, that in this case the neutrons originate from different times at the source, which might reduce the usable bandwidth as seen in Fig. 3, where the trajectories of the longest wavelength neutrons originate from  $t < 0$ .

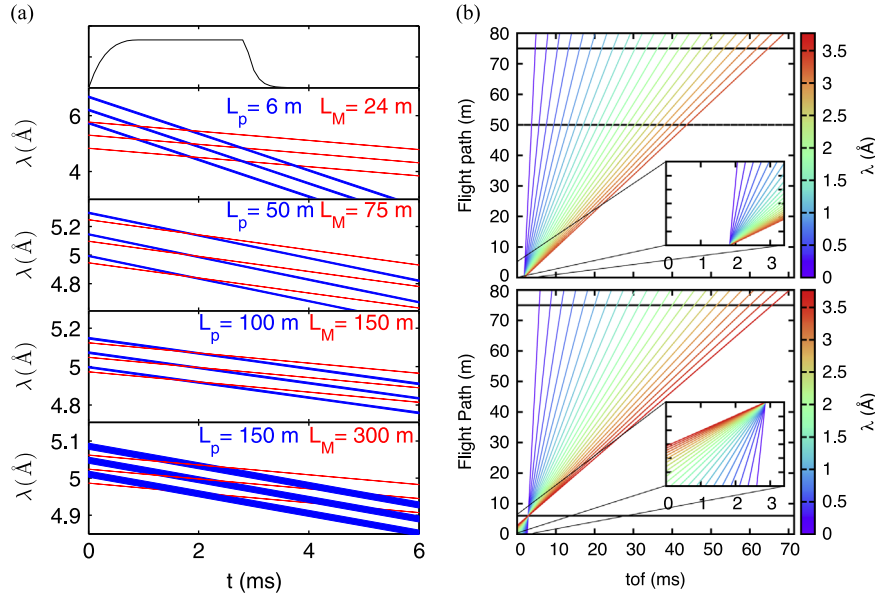


**Fig. 3.** (a) Acceptance diagram for P and M choppers at different distances from the moderator surface  $L_P$  and  $L_M$ , respectively. The opening times of the choppers are balanced according to Eq. (6) for  $\lambda' = \lambda$ . Red: accepted by the M chopper; blue: accepted by the P chopper. Two more accepted regions are shown for the M chopper, corresponding to the opening one revolution before and after, respectively. The top most panel represents the pulse shape of the ESS moderator. An afterglow is expected up to 6 ms after the beginning of the pulse. The frequency of the M chopper is 350 Hz, the repetition rate of the P chopper is given by Eq. (9). (b) A flight-path-diagram showing the difference between having the P chopper close to the source (bottom) or having it at larger distance fulfilling condition Eq. (9) (top). The insets focus short time-of-flight close to the moderator surface. (For interpretation of the references to color in this figure caption, the reader is referred to the web version of this paper.)

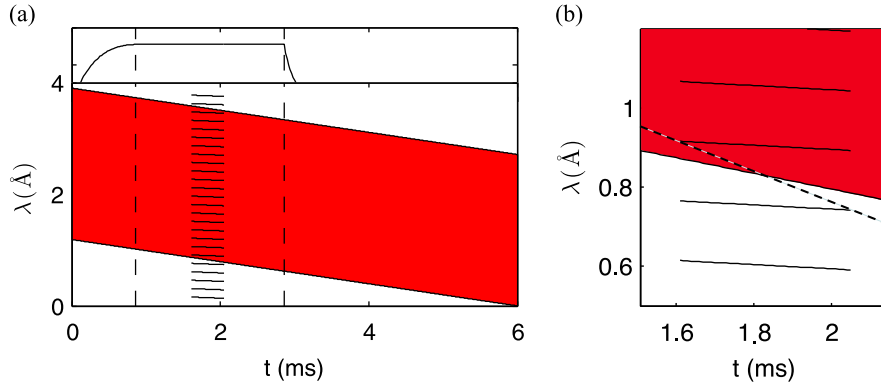


**Fig. 4.** Acceptance diagrams for the bandwidth selection for the time the moderator emits neutrons. The black lines give the regions accepted by the P and M choppers. The red region indicates, when the bandwidth chopper accepts neutrons. (a) Full acceptance region. (b) Zoom into the low wavelength limit region: the slope of the dashed line determines the minimum distance  $L_{BW}$ , at which the band width chopper can open exactly between two pulses defined the P and M choppers, neglecting the finite opening time. (For interpretation of the references to color in this figure caption, the reader is referred to the web version of this paper.)

#### 4. Bandwidth selection

The neutron source does not only emit neutrons in the wavelength band given by Eq. (7). Therefore the chopper system must be extended to limit the bandwidth that is used from a single source pulse. For the specification of the bandwidth chopper system we analyze the acceptance diagram Fig. 4: The red region in Fig. 4 indicates the full acceptance regions of the bandwidth chopper at  $L_{BW} = 30$  m. The zoom in Fig. 4b clarifies, how this distance was determined: the slope of the acceptance regions is inversely proportional to the distance of the respective chopper from the moderator surface. The dashed line determines the shortest distance  $L_{BW}$ , where the bandwidth chopper is fully open for one pulse of the P, M chopper system and fully closed for the preceding pulse. In that case we do not take into account the finite time to open the neutron guide cross-section at the band width chopper position. Therefore, the bandwidth chopper is placed at a larger distance from the moderator, indicated by the flatter slope

in the acceptance diagram. The transmitted bandwidth is then determined by the opening of the chopper. A variable bandwidth selection can be obtained implementing this chopper by two discs with  $180^\circ$  windows. The bandwidth can then be selected by the phase between the choppers, which allows us to vary the chopper opening between 0 and  $180^\circ$ .

To avoid contamination from earlier spallation pulses, the action of this bandwidth chopper is not sufficient. It is necessary to have any other system of two choppers, that has a bandwidth smaller than the repeat wavelength of the bandwidth chopper. For the layout presented in Fig. 3 that condition is fulfilled, if the P chopper pair is constructed with a finite spacing such that

$$4\tau_P \times 14 \text{ Hz} < \frac{L_{P_1 P_2}}{L_{BW}}. \quad (10)$$

The factor 4 assures that the extreme wavelengths passing through the P chopper pair are considered. If  $\tau_P$  becomes larger due to a larger distance  $L_{PM}$  (cf. Eq. (6)), it might be necessary to add

another slow chopper, which builds such a chopper system in combination with the first bandwidth chopper.

## 5. Adapted time frames

The time frame requested by the experiment is set by the time the energy loss neutrons need to arrive at the detector.

$$T_{\text{frame}} = \frac{m_n}{h} L_{\text{SD}}, \quad \lambda' = \frac{m_n}{h} L_{\text{SD}} \lambda \sqrt{\frac{1}{\frac{\hbar\omega}{E} + 1}} \quad (11)$$

Here  $\hbar\omega$  denotes the energy transfer to the sample during the scattering process and  $E$  the initial neutron energy. The time necessary to collect the full energy spectrum of the sample depends on the accessible excitations. In the thermal energy range high energy excitations require a large energy window. If the energy of the neutrons is not high enough to create excitations in the sample, the time frames can be shortened as frame overlap between energy loss events from the one pulse and energy gain processes from the subsequent pulse is excluded. However, a general condition for the length of the time frame and hence the repetition rate cannot be given, as it depends on the excitation spectrum of the specific sample under investigation.

In contrast to this request for variable time frames the M-chopper spinning at the constant frequency  $f_M$  sets a fixed long wavelength limit, if the time frame is limited by the time, at which two subsequent pulses reach the sample position:

$$0 \text{ \AA} < \lambda' < \frac{f_M^{-1} - \delta\lambda L_{\text{MS}}}{L_{\text{SD}}}. \quad (12)$$

Therefore the chopper system must be flexible enough to shift the long wavelength limit, if the neutron energy loss increases the wavelength beyond that limit.

We describe here a new chopper concept, the so-called fan chopper, which selectively suppresses the pulses that are prepared by the P and M choppers. This pulse suppression chopper consists of several narrow blades, which spin at the source frequency (14 Hz for ESS). Spinning a blade of the specified width  $d_{\text{blade}}$  and radius  $R_{\text{sup}}$  with 14 Hz, any single pulse can be suppressed by choice of the phase. For the suppression of several pulses, several blades can be mounted on the same axle, where the phases of the blades can be set independently. A schematic drawing of the chopper is given in Fig. 5, where different blades are connected to

hollow shafts, driven on a common axle. In the flight-path-diagram Fig. 5a the fan chopper suppresses four M chopper pulses, to have sufficient recording time for neutrons with  $\lambda' < 1.5 \times \lambda$ . While the blades in the example have been phased to suppress 4 pulses that could pass through the M chopper spinning at 350 Hz, there is no restriction to phase them according to an arbitrary frequency of the M chopper, e.g. if the M chopper frequency is varied to adapt the energy resolution. It should be emphasized that there is no limitation, which pulse can be suppressed. As an example consider a narrow high energy excitation, which is just beyond the limits of the time frame set by Eq. (11) for a pulse with energy  $E$ . The subsequent lower energy neutrons cannot excite high enough, so the time frame can be shorter for the colder neutrons without risking frame overlap in such a special case.

The blade width  $d_{\text{sup}}$  can be calculated from the following relations:

$$\frac{2}{f_M} - \frac{d_{\text{sup}} + d_{\text{NG}}}{\omega_{\text{sup}} R_{\text{sup}}} > \tau_M \quad (13)$$

$$\frac{d_{\text{sup}} - d_{\text{NG}}}{\omega_{\text{sup}} R_{\text{sup}}} > \tau_M \quad (14)$$

$d_{\text{sup}}$  and  $d_{\text{NG}}$  give the width of a single chopper blade and the neutron guide at the chopper position, respectively,  $\omega_{\text{sub}} = 2\pi f_{\text{source}}$  is the angular velocity of the fan chopper and  $R_{\text{sup}}$  is the distance from the chopper axle to the inner edge of the neutron guide window.  $f_M$  and  $\tau_M$  are the frequency and the burst time of the M chopper, respectively. Expression Eq. (13) confirms that the pulses before and after the suppressed pulse are not affected. Expression Eq. (14) takes care that the transmission of the chopper is exactly zero during the time at which the neutrons could be transmitted through the M chopper.

## 6. TO chopper

As mentioned earlier during and after the interaction with the proton beam a lot of high energetic particles are released from the moderator. These particles are a serious potential origin of background for the experiment. The situation at a long pulse spallation source is more severe as the production time of high energy

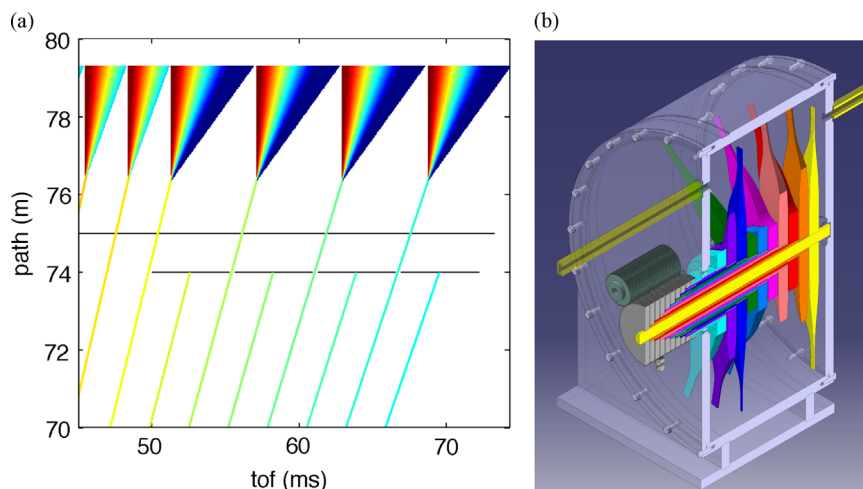


**Fig. 5.** (a) Zoom into the flight-path-diagram Fig. 1 clarifying the principle of the fan chopper: 2 periods of the M chopper are available for closing and opening the neutron beam and 100% absorption must be assured, when the M chopper is open. Here the blades are fanned out to block 4 pulses resulting in 4 time frames covering an extended  $\lambda'$  range. (b) Schematic of the engineering realization: the chopper has a repetition rate of 14 Hz. Each blade can be phased independently.

particles, i.e. the proton pulse duration, is a significant fraction of the source periodicity.

If the moderator-to-detector distance is increased and the direct line-of-sight is avoided by the neutron transport system, this background contribution can be reduced. The brilliance transfer of instruments aiming for a broad bandwidth and high neutron energies is, however, restricted for short neutron guides.

Alternatively, the direct line-of-sight can be blocked during the impact of the proton beam by a T0 chopper. This chopper must be very massive to stop a significant amount of the high energy particles, especially the fast neutrons. As an example, choppers in use at the SNS or in J-Parc bring 30 cm of steel into the beam. At the long pulse source the choppers must close the beam completely for 5–7 ms. In Fig. 1 we show the impact of closing the direct-line-of-sight for 6 ms, i.e. the neutron guide is completely blocked during this time and the time for opening and closing the beam has to be added, when the effect of the chopper is investigated. This long closing time leads to significant black regions in the neutron spectrum, which is not accessible for an experiment. As shown in Fig. 1 only neutrons above a certain wavelength can pass the chopper, depending on the departure of the neutrons from the moderator. In the figure we have assumed that the neutrons used at the spectrometer originate from the center of the plateau phase of the neutron time distribution. Furthermore, the chopper will create also black regions for other bands. This is shown in the acceptance diagram of the T0 chopper in Fig. 6. The black regions indicate regions blocked by the chopper. The dashed lines indicate the region, from which the neutrons for the experiment originate. We compare in the top and bottom figure two different realizations of a T0 chopper. The lower graph consists of a single blade as in operation at the short pulse sources spinning at 14 Hz. In this case the angular width of the blade is determined by the angular width of the neutron guide  $\beta$ , the time  $T_0$  and the angular velocity of the T0 chopper:

$$\alpha = \beta + T_0 \times \omega_{T_0} \quad (15)$$

The center graph displays the acceptance diagram for two counter rotating blades also spinning at 14 Hz. As long as  $\alpha > \beta$

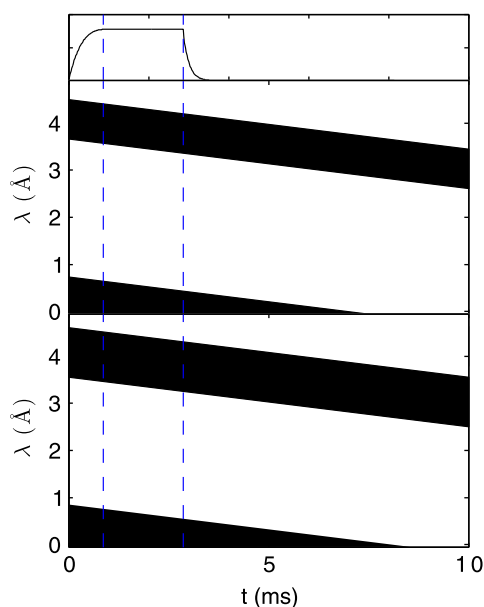


**Fig. 6.** Acceptance diagrams for a T0 chopper. (Top) ESS pulse shape. (Center) counter rotating chopper blades at  $L_{T_0} = 37.5$  m. (Bottom) single chopper blade at the same position. Black regions indicate reduced transmission. The blades are dimensioned to have zero transmission for 6 ms. The chopper frequency is 14 Hz in both cases. The chopper has to opposite blades to be balanced, yielding a repetition rate of 28 Hz.

it is now sufficient, if

$$\alpha = T_0 \times \omega_{T_0}. \quad (16)$$

As a result the upper configuration transmits a larger bandwidth. Particularly the lower limit is shifted to a lower wavelength. For the distance of 37.5 m the lower limit of the second black region coincides with the bandwidth. For the counter rotating blades, the thickness of a single blade cannot be reduced, because for some time only a single blade is in the beam.

## 7. Conclusion

We have addressed the different aspects of a chopper system for a direct geometry time-of-flight spectrometer at a long pulse spallation source. We analyze the acceptance diagrams of the various choppers used at the spectrometer to determine the time and wavelength, at which the source emits neutrons that pass through the chopper system.

The long pulse nature of the source provides the freedom to vary the resolution in a wide range by the P and M chopper speed and windows. If the instrument is optimized for good energy resolution, the distance between the P and M chopper should be larger than 20 m.

The special feature of a chopper spectrometer at a pulsed source is the multi-chromatic operation, i.e. the employment of multiple initial wavelengths. On a long pulse source one can choose between a broad or narrow bandwidth operation, as the moderator time distribution is not determining the energy resolution. The overall length from source to detector determines the dynamical range that can be probed. The band width selection can be accomplished by a single chopper taking the acceptance properties of the P and M chopper system into account. Furthermore the distance between the moderator surface and the M chopper determines the energy step in multi-chromatic operation.

To explore the large dynamic range optimally it is important to adapt the time frame according to the requested energy transfer range. A novel ‘fan chopper’ design provides the opportunity for arbitrary pulse suppression to increase the time frame.

A special effort is required to prevent an increased background level due to the long impact of the proton beam onto the target and the related high energy particle production. Besides the option discussed in this paper, it is furthermore possible to use a neutron transport system, which omits the line-of-sight from the sample region to the source and increases the distance.

Chopper spectroscopy at a long pulse spallation source offers unique possibilities to study the dynamics in condensed matter as unprecedented energy resolution at thermal and cold neutron energies can be combined in a single experiment with high flux measurements. The multi-chromatic operation already used at short pulse sources can be explored more efficiently, as all parameters such as energy resolution and dynamic range are controlled by the chopper system without constraints by the source characteristic.

## Acknowledgments

This work was funded by the BMBF through the collaborative project 05E10CJ1.

## References

- [1] F. Mezei, M. Russina, Multiplexing chopper systems for pulsed neutron source instruments, in: Proceedings of the SPIE—The International Society for Optical Engineering, vol. 4785, SPIE, Seattle, WA, USA, 2002, pp. 24–33. doi:<http://dx.doi.org/10.1117/12.451687>.

- [2] M. Nakamura, R. Kajimoto, Y. Inamura, F. Mizuno, M. Fujita, T. Yokoo, M. Arai, *Journal of the Physical Society of Japan* 78 (9) (2009) 093002, <http://dx.doi.org/10.1143/JPSJ.78.093002>.
- [3] R.E. Lechner, Optimization of a multi-disk chopper spectrometer for cold neutron scattering experiments, in: M. Misawa, M. Furusaka, H. Ikeda, N. Watanabe (Eds.), *Proceedings ICANS-IX*, KEK, 1991.
- [4] S.V. Roth, *Konzeption und neutroneoptische optimierung des kalten flugzeit-spektrometers am frm-ii* (Ph.D. thesis), TU München, 2001.
- [5] J. Copley, *Nuclear Instruments and Methods in Physics Research Section A: Accelerators, Spectrometers, Detectors and Associated Equipment* 273 (1) (1988) 67 [http://dx.doi.org/10.1016/0168-9002\(88\)90800-5](http://dx.doi.org/10.1016/0168-9002(88)90800-5), URL (<http://www.sciencedirect.com/science/article/pii/0168900288908005>).
- [6] M. Russina, F. Mezei, *Journal of Physics: Conference Series* 251 (2010) 012079, <http://dx.doi.org/10.1088/1742-6596/251/1/012079>.
- [7] M. Russina, F. Mezei, *Nuclear Instruments and Methods in Physics Research Section A: Accelerators, Spectrometers, Detectors and Associated Equipment* 604 (3) (2009) 624 <http://dx.doi.org/10.1016/j.nima.2009.03.010>, URL (<http://www.sciencedirect.com/science/article/pii/S0168900209004252>).
- [8] M. Nakamura, K. Nakajima, R. Kajimoto, M. Arai, *Journal of Neutron Research* 15 (1) (2007) 31, <http://dx.doi.org/10.1080/10238160601048767>.
- [9] J.R.D. Copley, *Nuclear Instruments and Methods in Physics Research Section A: Accelerators, Spectrometers, Detectors and Associated Equipment* 510 (3) (2003) 318 [http://dx.doi.org/10.1016/S0168-9002\(03\)01731-5](http://dx.doi.org/10.1016/S0168-9002(03)01731-5), URL (<http://www.sciencedirect.com/science/article/pii/S0168900203017315>).
- [10] K. Andersen, *Journal of Neutron Research* 10 (3) (2002) 179, <http://dx.doi.org/10.1080/1023816021000020635>.
- [11] H. Schober, Ch. Losert, F. Mezei, J.C. Cook, *Journal of Neutron Research* 8 (3) (2000) 175.